Development and validation of an integrated system for lung cancer screening and post-screening pulmonary nodules management: a proof-of-concept study (ASCEND-LUNG)

Yichen Jin,[a,b,k] Wei Mu,[c,d,k] Yezhen Shi,[e,k] Qingyi Qi,[f,k] Wenxiang Wang,[a,b,k] Yue He,[a,b,k] Xiaoran Sun,[e] Bo Yang,[e] Peng Cui,[e] Chengcheng Li,[e] Fang Liu,[e] Yuxia Liu,[e] Guoqiang Wang,[e] Jing Zhao,[e] Yuzi Zhang,[e] Shuaitong Zhang,[g] Caifang Cao,[c,d] Chao Sun,[f] Nan Hong,[f] Shangli Cai,[e,**] Jie Tian,[c,d,h,***] Fan Yang,[a,b,****] and Kezhong Chen[a,b,i,j,*]

[a]Department of Thoracic Oncology Institute & Research Unit of Intelligence Diagnosis and Treatment in Early Non-small Cell Lung Cancer, Peking University People's Hospital, Beijing, 100044, China
[b]Department of Thoracic Surgery, Peking University People's Hospital, Beijing, 100044, China
[c]School of Engineering Medicine, Beihang University, Beijing, 100191, China
[d]Key Laboratory of Big Data-Based Precision Medicine (Beihang University), Ministry of Industry and Information Technology of the People's Republic of China, Beijing, 100191, China
[e]Burning Rock Biotech, Guangzhou, 510300, China
[f]Department of Radiology, Peking University People's Hospital, Beijing, 100044, China
[g]School of Medical Technology, Beijing Institute of Technology, Beijing, 100081, China
[h]CAS Key Laboratory of Molecular Imaging, Institute of Automation, Chinese Academy of Sciences, Beijing, 100191, China
[i]Institute of Advanced Clinical Medicine, Peking University, Beijing, 100191, China

eClinicalMedicine
2024;75: 102769
Published Online xxx
https://doi.org/10.1016/j.eclinm.2024.102769

Summary

Background In order to address the low compliance and dissatisfied specificity of low-dose computed tomography (LDCT), efficient and non-invasive approaches are needed to complement its limitations for lung cancer screening and management. The ASCEND-LUNG study is a prospective two-stage case–control study designed to evaluate the performance of a liquid biopsy-based comprehensive lung cancer screening and post-screening pulmonary nodules management system.

Methods We aimed to develop a comprehensive lung cancer system called Peking University Lung Cancer Screening and Management System (PKU-LCSMS) which comprises a lung cancer screening model to identify specific populations requiring LDCT and an artificial intelligence-aided (AI-aided) pulmonary nodules diagnostic model to classify pulmonary nodules following LDCT. A dataset of 465 participants (216 cancer, 47 benign, 202 non-cancer control) were used for the two models' development phase. For the lung cancer screening model development, cancer participants were randomly split at a ratio of 1:1 into the train and validation cohorts, and then non-cancer controls were age-matched to the cancer cases in a 1:1 ratio. Similarly, for the AI-aided pulmonary nodules model, cancer and benign participants were also randomly divided at a ratio of 2:1 into the train and validation cohorts. Subsequently, during the model validation phase, sensitivity and specificity were validated using an independent validation cohort consisting of 291 participants (140 cancer, 25 benign, 126 non-cancer control). Prospectively collected blood samples were analyzed for multi-omics including cell-free DNA (cfDNA) methylation, mutation, and serum protein. Computerized tomography (CT) images data was also obtained. Paired tissue samples were additionally analyzed for DNA methylation, DNA mutation, and messenger RNA (mRNA) expression to further explore the potential biological mechanisms. This study is registered with ClinicalTrials.gov, NCT04817046.

Findings Baseline blood samples were evaluated for the whole screening and diagnostic process. The cfDNA methylation-based lung cancer screening model exhibited the highest area under the curve (AUC) of 0.910 (95% CI, 0.869–0.950), followed by the protein model (0.891 [95% CI, 0.845–0.938]) and lastly the mutation model (0.577 [95% CI, 0.482–0.672]). Further, the final screening model, which incorporated cfDNA methylation and protein features,

*Corresponding author. Department of Thoracic Oncology Institute & Research Unit of Intelligence Diagnosis and Treatment in Early Non-small Cell Lung Cancer, Peking University People's Hospital, Beijing, 100044, China.
**Corresponding author.
***Corresponding author. Department of Engineering, School of Engineering Medicine, Beihang University, Beijing, China.
****Corresponding author. Department of Thoracic Oncology Institute & Research Unit of Intelligence Diagnosis and Treatment in Early Non-small Cell Lung Cancer, Peking University People's Hospital, Beijing, 100044, China.
E-mail addresses: mdkzchen@163.com (K. Chen), shangli.cai@brbiotech.com (S. Cai), tian@ieee.org (J. Tian), yangfan@pkuph.edu.cn (F. Yang).
[j]Lead contact.
[k]These authors contributed equally to this work.

achieved an AUC of 0.963 (95% CI, 0.942–0.984). In the independent validation cohort, the multi-omics screening model showed a sensitivity of 99.2% (95% CI, 0.957–1.000) at a specificity of 56.3% (95% CI, 0.472–0.652). For the AI-aided pulmonary nodules diagnostic model, which incorporated cfDNA methylation and CT images features, it yielded a sensitivity of 81.1% (95% CI, 0.732–0.875), a specificity of 76.0% (95% CI, 0.549–0.906) in the independent validation cohort. Furthermore, four differentially methylated regions (DMRs) were shared in the lung cancer screening model and the AI-aided pulmonary nodules diagnostic model.

Interpretation We developed and validated a liquid biopsy-based comprehensive lung cancer screening and management system called PKU-LCSMS which combined a blood multi-omics based lung cancer screening model incorporating cfDNA methylation and protein features and an AI-aided pulmonary nodules diagnostic model integrating CT images and cfDNA methylation features in sequence to streamline the entire process of lung cancer screening and post-screening pulmonary nodules management. It might provide a promising applicable solution for lung cancer screening and management.

Funding This work was supported by Science, Science, Technology & Innovation Project of Xiongan New Area, Beijing Natural Science Foundation, CAMS Innovation Fund for Medical Sciences (CIFMS), Clinical Medicine Plus X-Young Scholars Project of Peking University, the Fundamental Research Funds for the Central Universities, Research Unit of Intelligence Diagnosis and Treatment in Early Non-small Cell Lung Cancer, Chinese Academy of Medical Sciences, National Natural Science Foundation of China, Peking University People's Hospital Research and Development Funds, National Key Research and Development Program of China, and the fundamental research funds for the central universities.

Copyright © 2024 Published by Elsevier Ltd. This is an open access article under the CC BY-NC-ND license (http://creativecommons.org/licenses/by-nc-nd/4.0/).

Keywords: Lung cancer screening; Cell-free DNA; Methylation; LDCT; Pulmonary nodules

Research in context

Evidence before this study

Low-dose computed tomography (LDCT) screening has shown significant association with a reduction in lung cancer mortality in randomized clinical trials, but its widespread use faces challenges such as low compliance. Additionally, accurately classifying pulmonary nodules is also crucial after LDCT screening. For the first time, we have designed this case–control study to investigate the use of liquid biopsy in integrating two distinct clinical scenarios: LDCT screening and post-LDCT pulmonary nodule management. We searched PubMed up to December 31, 2023, using the terms ("lung cancer") AND ("screening" OR "pulmonary nodules") AND ("liquid biopsy" OR "cfDNA" OR "ctDNA") with no language restrictions. Previous studies have solely focused on specific populations within only one scenario.

Added value of this study

The ASCEND-LUNG (AssesSment of early-deteCtion basEd oN liquiD biopsy, NCT04817046) study is a prospective case–control study aimed at establishing and validating a multi-omics screening and management system including lung cancer screening and pulmonary nodules diagnostic functions. We have developed and validated a novel integrated liquid biopsy-based comprehensive system called Peking University Lung Cancer Screening and Management system (PKU-LCSMS). This system integrates a lung cancer screening model based on blood multi-omics assays used prior LDCT, along with an AI-aided pulmonary nodules diagnostic model that utilizes cfDNA methylation and chest CT images to accurately differentiate pulmonary nodules. Specifically, the baseline blood test used for screening can also serve for subsequent post-screening management of pulmonary nodules, ensuring a convenient and efficient process throughout.

Implications of all the available evidence

With the baseline blood sample as a central element, the PKU-LCSMS offers a promising solution for streamlining the entire process of lung cancer screening and post-screening pulmonary nodules management. Considering the substantial burden of lung cancer and pulmonary nodules in China and worldwide, the PKU-LCSMS has the potential to accurately identify populations requiring clinical intervention and significantly optimize the detection, diagnosis, and treatment of lung cancer.

Introduction

Low-dose computed tomography (LDCT) screening has shown significant association with a reduction in lung cancer mortality in randomized clinical trials, and it has been recommended for high-risk populations by the American Cancer Society.[1,2] However, the widespread implementation of LDCT in the clinical practice has challenges. Because of the low compliance and

accessibility to LDCT, it is reported that only 3.3%–3.9% of high risk populations have received LDCT for lung cancer screening between 2010 and 2015, according to the National Health Interview Study.[3] In addition, the suboptimal specificity of LDCT may lead to overdiagnosis and anxiety in populations identified with benign pulmonary nodules.[2] Not to mention that LDCT exposes individuals to radiation, which may increase the risk of cancers. Thus, there is an urgent need to develop a novel and efficient lung cancer screening and post-screening management system, which needs to meet the following requirements: (i) simple and convenient to ensure a high compliance; (ii) relatively high sensitivity; (iii) efficiently reducing the number of individuals undergoing LDCT screenings; (iv) effectively distinguishing between benign and malignant lung nodules to minimize unnecessary invasive diagnostic biopsies or surgeries.

Liquid biopsy, widely acknowledged for its minimal invasiveness and convenience,[4–7] has a natural advantage in effectively addressing the issues present in the current lung cancer screening and management system based on LDCT.[8–10]

Firstly, the convenience of liquid biopsy may help to solve the poor adherence of LDCT. A liquid biopsy-based assay with relatively high sensitivity and acceptable specificity can be used prior to LDCT to reduce unnecessary LDCT usage. Recently, cell-free DNA (cfDNA) based biomarkers for screening have shown promise in improving the accuracy of cancer detection by capturing the comprehensive molecular and (epi) genetic characteristics of tumors, overcoming intra-tumor heterogeneity. However, sensitivity in early-stage adenocarcinoma may be constrained by low levels of cfDNA.[11,12] For instance, technologies such as CAPP-seq-based Lung Clip[8] and genome-wide cfDNA fragmentation-based DELFI[9] have demonstrated impressive performance in lung cancer. Nonetheless, the sensitivity for detecting stage I cancers has been restricted to around 40–60%. Other biomarkers, such as proteins,[13,14] autoantibodies,[15] and RNA,[16–18] have also demonstrated potential for lung cancer detection, but some may face challenges related to suboptimal performance or the need for stable sample handling. Given the differences in the sources, generation, and release mechanisms of various biomarkers, there may be a degree of complementarity among them. Therefore, integrating multi-omics data from liquid biopsy has the potential to address single-source limitations and improve the performance of cancer detection.

Secondly, accurately classifying pulmonary nodules is crucial after lung cancer screening. Approximately 22.9% of high-risk individuals have positive LDCT screening results, with about 59.6% of them having pulmonary nodules measuring 5 mm or larger.[19] Several studies have focused on investigating the potential of cfDNA as a biomarker for differentiating pulmonary nodules, with cfDNA methylation being the mainstream technique. These studies have reported sensitivities ranging from 56.9% to 91% and specificities from 61% to 91%.[10] Furthermore, radiomics analysis has also emerged as a powerful tool for extracting high-throughput quantitative features from non-invasive medical images with artificial intelligence (AI) algorithms. This method uncovers hidden micro-information and correlates well with pathology results.[20] The development of the LDCT image-based deep learning algorithm, known as Sybil, has shown promising specificity in reducing false-positive rate among patients with pulmonary nodules.[21] To further enhance the performance, the integration of liquid biopsies, specifically cfDNA methylation, along with radiomics, has the potentially to improve the diagnostic capabilities.[22–25]

Herein, in order to optimize the LDCT screening pathway and enhance the accuracy of distinguishing between benign and malignant pulmonary nodules found during LDCT screening, we have developed and validated a novel integrated liquid biopsy-based comprehensive system called Peking University Lung Cancer Screening and Management System (PKU-LCSMS). This system integrates a lung cancer screening model based on blood multi-omics assays, along with an AI-aided pulmonary nodules diagnostic model that utilizes cfDNA methylation and Chest CT images to accurately differentiate pulmonary nodules. This innovative system is designed to streamline the entire process of lung cancer screening and post-screening pulmonary nodules management. It has the potential to optimize lung cancer screening and management by providing a practical and effective solution.

Methods

Study design and participants

The ASCEND-LUNG (AssesSment of early-deteCtion basEd oN liquiD biopsy, NCT04817046) study is a prospective case–control study aimed at establishing and validating a multi-omics screening and management system including lung cancer screening and pulmonary nodules diagnostic functions (Fig. 1A). Participants with pathologically diagnosed lung cancer or benign pulmonary nodules were enrolled in the present study and pre-treatment or pre-diagnosis blood samples were obtained from each participant. A total of 280 participants (228 cancer, 52 benign) enrolled from the department of Thoracic Surgery of Peking University People's Hospital (PKUPH cohort) between February 2021 and March 2022 were used for model development (Fig. 1B). Another 187 participants (155 cancer, 32 benign) enrolled from the department of Thoracic Oncology Institute & Research Unit of Intelligence Diagnosis and

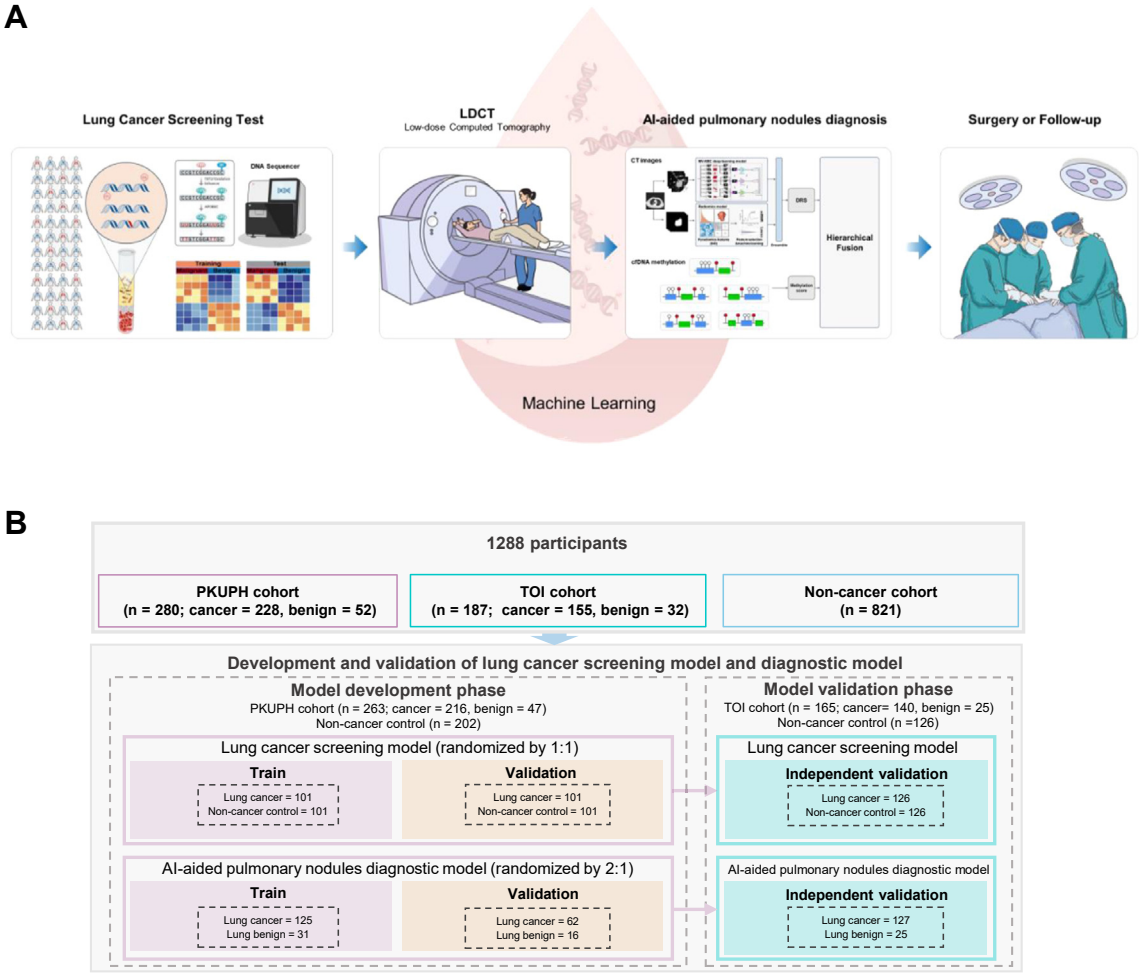

Fig. 1: **The workflow diagram of PKU-LCSMS**. **(A)** The workflow diagram illustrated the process of the Peking University Lung Cancer Screening and Management System (PKU-LCSMS). This system comprised a lung cancer screening model utilized prior to low-dose computed tomography (LDCT), and an artificial intelligence-aided (AI-aided) pulmonary nodules diagnostic model to classify pulmonary nodules post LDCT screening. The construction of the lung cancer screening model was based on the multi-omics blood test, combining cell-free DNA (cfDNA) methylation and serum proteins. The construction of the AI-aided pulmonary nodules diagnostic model was based on radiomics and cfDNA methylation data. Firstly, the screening populations undergoes a blood test for lung cancer screening, and individuals with a positive results of the blood test will proceed to further LDCT examination. Those without positive findings of LDCT can opt for a blood test next year for the potential identification at that time. Secondly, the population identified with pulmonary nodules through LDCT screening further undergoes the AI-aided pulmonary nodules diagnostic model to assess their risk, assisting in guiding subsequent decisions. **(B)** Flowchart of participant selection in three cohorts. A total of 1288 participants were included in the study including 280 participants from the PKUPH cohort, 187 participants from the TOI cohort, and 821 control participants from another non-cancer control cohort. The PKUPH cohort was used for model development and the TOI cohort was used as an independent validation cohort. More details were provided in Supplementary Fig. S1. PKUPH: the department of Thoracic Surgery of Peking University People's Hospital; TOI: the department of Thoracic Oncology Institute of Peking University People's Hospital.

Treatment in Early Non-small Cell Lung Cancer of Peking University People's Hospital (TOI cohort) between March 2022 and August 2022 were used as an independent validation cohort (Fig. 1B). More details were provided in Supplementary Fig. S1 and Supplementary Materials.

To minimize the potential bias from age-related factors on the lung cancer screening model,[26] age-matched non-cancer controls from a community-based cohort (NCT04972201) were employed using a 1:1 randomization stratified matching approach[27] (Supplementary Fig. S1). All non-cancer controls received LDCT examinations to confirm the absence of lung cancer or nodules with a diameter greater than or equal to 6 mm. Additional examinations, including visceral ultrasound, mammography for females, blood

tests, and urine tests, were also conducted for the non-cancer controls to rule out cancer in other organs. Non-cancer controls were followed up for at least one year and any cancer occurred during follow-up would be excluded. An analyst was responsible for conducting the random split of the dataset. When the model was locked for the independent validation, another analyst blind to the clinical data of the independent validation cohort was assigned for data generation and processing.

Ethics statement

The study was approved by the Ethics Committee of Peking University People's Hospital (2021PHB029-001). The study was performed in accordance with the Declaration of Helsinki and Good Clinical Practice. All participants provided written informed consent before participation. The trial is registered with ClinicalTrials.gov (No. NCT04817046).

Sample collection, storage and process

In this study, pre-treatment or pre-diagnosis blood samples were collected from each participant. For each individual's blood sample collection, 8–10 mL blood was collected using a Cell-Free DNA BCT tube (Streck) for the purposes of plasma cfDNA extraction. Plasma cfDNA extraction was performed using the QIAamp Circulating Nucleic Acid Kit (Qiagen). Additionally, 8–10 mL blood was collected using serum tube for the detection of 16 tumor protein markers. More details were provided in Supplementary Materials. Furthermore, subsets of cancer tissue samples and adjacent tissues were obtained.

The multi-omics blood test

A methylation panel of 498,713 CpG sites sequenced was performed on cfDNA samples with an average sequencing depth of 1000X. The target libraries were quantified by real-time PCR and sequenced on Illumina NovaSeq 6000. To enhance the accuracy of differentially methylated regions (DMR) detection, we employed a method called methylation block score (MBS) that defines CpG sites based on both the close genomic distance and highly correlated methylation levels of CpG sites.[28] The definition of MBS is provided in Supplementary Materials. About 10 ng of plasma cfDNA samples were subjected to the targeted methylation panel. For samples that had remaining cfDNA beyond 10 ng, the OncoCompass Target panel, consisting of unique molecular identifier (UMI)-tagged 168 cancer-related genes,[29] was applied at a depth of 35,000X. To exclude the clonal hematopoiesis and germline mutations, the 168 gene panel was also applied to white blood cells (WBC) with a depth of 10,000X. Furthermore, to minimize false positive results, additional filters were implemented to eliminate technical artifacts and errors arising from biological background. Specifically, readings with low comparison quality, unclear mapping, or improper pairing were removed from the original file (.bam). Non-reference alleles with low sequencing scores (Phred quality filtering score <30) or located within error-prone genomic regions, such as collateral/repetitive sequences, were excluded from further analysis.[30] Sixteen tumor protein markers were tested on the serum samples using Electrochemiluminescence method of Roche platform and fully automated chemiluminescence immunoassay system C2000 of Hotgen.

The multi-omics tissue sequence

All formalin-fixed paraffin-embedded (FFPE) tissues underwent a second research histopathology review conducted by an independent expert pathologist. Tumor tissues that contained less than 30% cancer cells or failed to meet the DNA or RNA quality control (QC) criterion were excluded from the subsequent sequencing. DNA and RNA from FFPE samples was extracted using the AllPrep DNA/RNA Mini Kit (Qiagen), according to the manufacturer's protocol. DNA and RNA quality and quantity were assessed using Qubit 4.0 (Thermo Scientific) and LabChip GXII touch 24 (PerkinElmer), respectively. Deep targeted bisulfite sequencing was performed on tissue DNA covering 498,713 CpG sites with an average sequencing depth of 500X to discover lung cancer specific CpG sites for model development. Furthermore, the 520 cancer-related genes (OncoScreen Plus, Burning Rock Biotech, Guangzhou, China) were captured and sequenced on the Illumina Nextseq 600 sequencer with an average depth of 1000X. Library preparation of mRNA were using VAHTSTM Stranded mRNA-seq Library Prep Kit for Illumina and VAHTSTM Total RNA-seq (H/M/R) Library Prep Kit for Illumina, respectively. Then RNA libraries were sequenced using the Illumina Novaseq 6000 S4.

Lung cancer screening model development and validation

Lung cancer participants and non-cancer controls were included in the development and validation of the lung cancer screening model. The construction of the model involved feature selection and model training. During the feature selection stage, the lung cancer specific DMRs were identified by comparing the cancer and adjacent tissues. The *P* values were generated using the Mann–Whitney U test and then adjusted for multiple tests using the Benjamini-Hochberg method. DMRs were defied as a mean difference greater than 0.2 and an adjusted *P* value less than 0.05. The protein data was transformed using the Box–Cox transformation to ensure a normal distribution. As for ctDNA, the presence or absence of mutations was directly utilized as a feature for the model.

In the model training stage, the methylation and protein models were constructed separately using 10-fold cross-validation and support vector machines (SVM) with a linear kernel. In the mutation model, any gene mutation detected was defined as a positive result. The performance of all three single-omics models including the methylation-based model, the protein-based model, and the mutation-based model, was evaluated by comparing their area under the curve (AUC) values. Subsequently, the multi-omics combined model was developed by integrating the output scores from single-omic models using the SVM method. All the analyses were performed using the scikit-learn library in Python version 3.9.7.

In the validation cohort and the independent validation cohort, we further evaluated the performance of the constructed multi-omics model by assessing AUC values, sensitivity, and specificity.

AI-aided pulmonary nodules diagnostic model development and validation

Participants with lung cancer and benign pulmonary nodules were included for the development and validation of the AI-aided pulmonary nodules diagnostic model. In summary, to comprehensively capture intratumor heterogeneity and the tumor microenvironment, we integrated pre-defined radiomics analysis and deep learning analysis into an AI-aided diagnostic model called Expert Plus. For the radiomics analysis, we extracted 876 features from each nodule and refined them using the mRMR and LASSO methods, which resulted in a Radiomics Signature (RS) comprising selected features weighted by coefficients derived from the LASSO method. Simultaneously, a deep learning model inspired by the multi-view knowledge-based collaborative deep learning network named MV-KBC model was developed.[31] Hyper images, generated from the cropped cube of the nodule, were processed using a residual Convolutional Neural Network (SResNet). By utilizing trainable weights, we calculated the weighted sum of SResNet outputs for each view to generate the Deep Learning Score (DLS), a predicted malignant probability score. The DLS and RS were used as covariates in a logistic regression model to obtain the CT-derived diagnostic risk score (DRS) (Fig. 1B).

Moreover, the hierarchical fusion method was proposed. To achieve high sensitivity and high specificity, we established two cutoff values for the CT-derived DRS in the train cohort. These cutoffs were referred to as the low threshold (Lth) and high threshold (Hth). Individuals scoring above the Hth were categorized as malignant, those scoring below the Lth were categorized as benign, and patients between the Hth and Lth thresholds were classified as intermediate risk. For those deemed at intermediate risk, additional assessment was conducted, incorporating cfDNA methylation markers through a multivariable logistic regression approach. The grid search method was employed to find the highest average AUC of the final fusion model during 5-fold cross-validation with the train cohort, and then the relative thresholds of sensitivity and specificity were determined. Comparisons between the AI-aided pulmonary nodules diagnostic model and classical mathematical models including the Mayo model[32] and Veterans Affairs (VA) model,[33] as well as clinical experts' judgement in the independent validation cohort were also conducted. More details are provided in Supplementary Materials.

Statistical analysis

All statistical analyses were performed using R version 3.6.0 and Python version 3.9.7. Categorical variables were presented as whole numbers, while continuous variables were presented as medians and interquartile ranges. Chi-square test was used for categorical variables. The Mann–Whitney U test was used to compare the differences in methylation block values between two groups, as well as mRNA expression levels. DeLong's test was conducted for the statistical comparison of AUCs. The continuous variables were described using the median and interquartile range, while the categorical variables were described with the count and percentage of occurrences. Visualizations such as volcano plot, heatmap, and Upset plot were generated using R pacakage 'ggplot2', 'ComplexHeatmap' and 'UpSetR', respectively. Ten-fold cross-validation SVM was carried out using Scikit-learn in Python. The AUC and 95% confidence interval (CI) were generated to assess the model performance, along with sensitivity, specificity, and accuracy. During the model development phase, AUC was employed to compare the performance of different models in order to select the optimal one. Following the identification of the optimal model, the performance of the independent validation cohort was assessed based on sensitivity and specificity. The 95% CIs for sensitivity and specificity were calculated with the Clopper-Pearson method. A two-sided P value less than 0.05 was considered statistically significant.

Role of the funding source

This study received funding from Science, Technology & Innovation Project of Xiongan New Area, Beijing Natural Science Foundation, CAMS Innovation Fund for Medical Sciences (CIFMS), Clinical Medicine Plus X-Young Scholars Project of Peking University, the Fundamental Research Funds for the Central Universities, Research Unit of Intelligence Diagnosis and Treatment in Early Non-small Cell Lung Cancer, Chinese Academy of Medical Sciences, National Natural Science Foundation of China, Peking University People's Hospital Research and Development Funds, National Key Research and Development Program of

China, and the fundamental research funds for the central universities. The funding was utilized for operation of platform-based trials, such as constructing Electronic Data Capture (EDC) systems for clinical trials, patient enrollment, and covering administrative costs. The funder had no role in study design, data collection, data analysis, data interpretation, or writing of the report.

Results

Patient characteristics

In this study, data from 328 cancer and 328 non-cancer control participants were used across the two phases for the lung cancer screening model development (train cohort and validation cohort) and model validation (independent validation cohort). In addition, chest CT images from 314 cancer and 72 CT-malignant-like benign pulmonary nodules were used for the AI-aided pulmonary nodules diagnostic model development (train cohort and validation cohort) and validation (independent validation cohort) (Fig. 1A). A total of 286 cancer cases overlapped between the lung cancer screening model (286/328, 87.2%) and the AI-aided pulmonary nodules diagnostic model (286/314, 91.1%), with 173 overlapped cancer cases in the model development phase and 113 cancer cases in the model validation phase. More details can be found in Supplementary Fig. S1 and Supplementary Materials.

The demographics and clinical characteristics of participants in the screening model and diagnostic model are summarized in Supplementary Tables S1 and S2, respectively. For marker selection, the methylation profiles of tissue samples were obtained from 35 lung cancers tissues and 33 adjacent tissues in the train cohort to identify lung cancer-specific methylation markers.

Methylation markers selection

In this study, we performed targeted methylation sequencing in lung cancer tissues (n = 35) and adjacent tissues (n = 33) from the train cohort. Distinct DNA methylation patterns between the samples were visualized in Fig. 2A. Totally, 1583 lung cancer-specific DMRs were identified (Fig. 2B). Of these DMRs, 654 (41.3%) were hypermethylated regions and 929 (58.7%) were hypomethylated regions in cancer. The methylation levels for the 1583 DMRs are depicted in the heatmap (Fig. 2C), exhibiting different methylation patterns between lung cancer and adjacent tissues.

As shown in the Sankey plot (Fig. 2D), the lung cancer-specific DMRs exhibited a higher proportion of hypermethylation in intergenic CpG islands (52.9%) and a higher proportion of hypomethylated DMRs in intergenic CpG islands (89.2%), and most of the DMRs were related with protein-coding (68.0% for hypermethylation and 63.9% for hypomethylation).

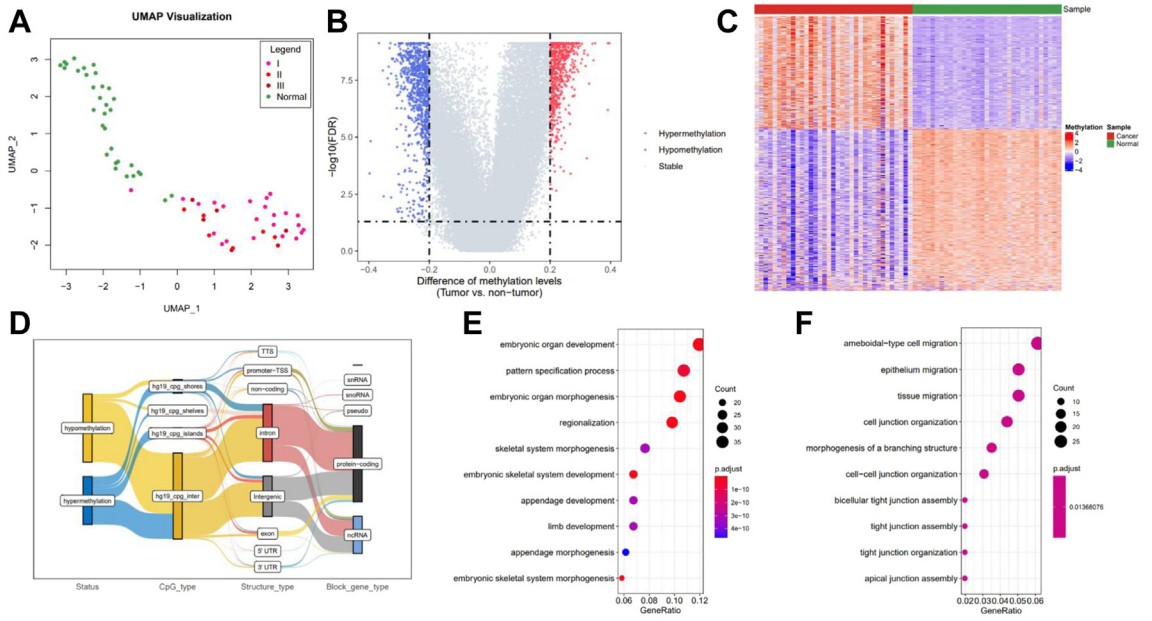

Fig. 2: **Tissue differentially methylation markers selection**. **(A)** UMAP visualization of methylated regions between cancer (n = 35) and adjacent (n = 33) tissues from the participants in the train cohort. **(B)** Volcano plot of DMRs between cancer (n = 35) and adjacent (n = 33) tissues. **(C)** Heatmap of DMRs in cancer and adjacent tissue. **(D)** Classification of DMRs in functional locations. In the GO enrichment analysis, top 10 up-regulated terms **(E)**, and top 10 down-regulated terms **(F)** were presented. UMAP, uniform manifold approximation and projection; DMRs, differentially methylated regions; GO, gene ontology.

Gene ontology (GO) enrichment analysis showed that the hypermethylated genes were enriched in the pathways involved in embryonic organ development and skeletal system morphogenesis (Fig. 2E), and the rest with hypomethylation levels in tumor tissues, enriched in the pathways related to epithelium migration, cell junction organization and tight junction assembly (Fig. 2F).

Construction and validation of the multi-omics based lung cancer screening model

We aimed to develop a lung cancer screening model with high sensitivity to be used before LDCT (Fig. 1A). Utilizing various omics data including cfDNA methylation, protein, and mutation, 202 cancers were randomly allocated in a 1:1 ratio to the train and validation cohorts, and then 202 non-cancer controls were age-matched to the cancer cases in a 1:1 ratio (Fig. 1B). The lung cancer-specific DMRs of cfDNA exhibited different methylation patterns between cancers and non-cancer controls in the train and validation cohorts (Fig. 3A). The mutation and tumor proteins landscapes in train and validation cohorts were also depicted in Fig. 3A. The cfDNA methylation lung cancer screening model performed best with AUC 0.910 (95% CI, 0.869–0.950) to discriminate lung cancers from non-cancer controls in the train cohort, while the protein and mutation yielded an AUC with 0.891 (95% CI, 0.845–0.938) and 0.577 (95% CI, 0.482–0.672), respectively (Fig. 3B). The sensitivities and specificities of different single-omic based lung cancer screening models in the train and validation cohorts are shown in Supplementary Table S3. To enhance the performance of the screening model, multi-omics combined model were evaluated. The performance of cfDNA methylation and protein integrated model outperformed the single cfDNA methylation model (AUC 0.963 vs. 0.910; DeLong's test, P = 0.0026). Moreover, there was no significant difference in AUCs between the three-omics detection model (cfDNA methylation + protein + ctDNA mutation) and the two-omics (cfDNA methylation + protein) detection model (AUC 0.969 vs. 0.963, P = 0.27). Since the ctDNA mutation contributed less to the performance of the screening model, it was not included in subsequently model development. The final multi-omics detection model (including cfDNA methylation and protein) yielded an AUC of 0.963 (95% CI, 0.942–0.984), 0.953 (95% CI, 0.927–0.979), and 0.966 (95% CI, 0.946–0.986) in the train, validation, and independent validation cohorts, respectively (Fig. 3C).

In the independent validation, with a specificity of 56.3% (95% CI, 47.2%–65.2%), the sensitivity of the multi-omics lung cancer screening model was 100% (95% CI, 95.1%–100%) for stage I, 100% (95% CI, 73.5%–100%) for stage II, and 100% (95% CI, 86.3%–100%) for stage III (Fig. 3D). The accuracy was 77.8% (95% CI, 82.5%–72.2%). The detailed sensitivities and specificities regarding different cohorts are shown in Supplementary Table S4. Moreover, there were also no significant differences of the AUCs in different subtypes in the independent validation cohorts (Fig. 3E–H).

Construction and validation of the AI-aided pulmonary nodules diagnostic model

We aimed to develop a pulmonary nodule diagnostic model based on Chest CT images data and cfDNA methylation to discriminate malignant nodules from benign nodules identified by LDCT (Fig. 1A).

The diagnostic model yielded AUCs of 0.875 (95% CI, 0.815–0.935), 0.834 (95% CI, 0.723–0.946) and 0.798 (95% CI, 0.694–0.902) in the train, validation, and independent validation cohorts to distinguish the malignant nodules from the benign nodules, respectively (Fig. 4A). The accuracy for the train, validation, and independent validation cohorts was 77.6% (95% CI, 83.4%–70.4%), 75.6% (95% CI, 83.8%–65.1%) and 80.3% (95% CI, 85.8%–73.2%) respectively. Differentiation between benign and malignant pulmonary nodules was achieved by a double scoring system (Fig. 4B). Firstly, the low-risk (predicted score $\leq$ –0.082), intermediate risk (–0.082 < predicted score < 2.571) and high-risk (predicted score $\geq$ 2.571) for CT-malignant-like nodules were defined according to the predicted scores from the DRS model. Participants categorized into low-risk and high-risk output the current results as the final conclusions, while the others with intermediate-risk were further classified using cfDNA methylation. The intermediate-risk populations in DRS model were further defined into low-risk (predicted score $\leq$ 0.297), intermediate-risk (0.297 < predicted score <0.774) and high-risk (predicted score $\geq$ 0.774) by the DRS-M model, based on images data and five cfDNA DMRs. The detailed information of the five DMRs were shown in Supplementary Table S5 and four of the five DMRs were also used in the lung cancer screening model. High-risk populations accounted for the majority of cancers (76.8%, 77.4%, and 81.1% in the train, validation, and independent validation cohorts, respectively) compared with benign patients (19.4%, 31.3%, and 24.0% in the train, validation, and independent validation cohorts, respectively) (Chi-square test, P < 0.001) (Fig. 4C). The risk remained high when stratified by different clinical covariates, even in the tumor with size less than 3 cm (77.4%), and in the stage I (76.9%) and stage II (92.9%) (Fig. 4D). The AI-aided pulmonary nodules diagnostic model had a higher fraction of cancers with timely diagnosis (81.1% [95% CI, 73.2%–87.5%]), compared with the Mayo model (48.0% [95% CI, 39.1%–57.1%]), the VA model (63.8% [95% CI, 54.8%–72.1%]), and three clinical experts' judgement (52.8%–76.4%) (Fig. 4E). Moreover, the diagnostic model showed a lower fraction of missed cancers diagnosis (0.8% [95% CI, 0%–4.3%]) compared to the Mayo model (13.4% [95% CI, 8.0%–20.6%]), the

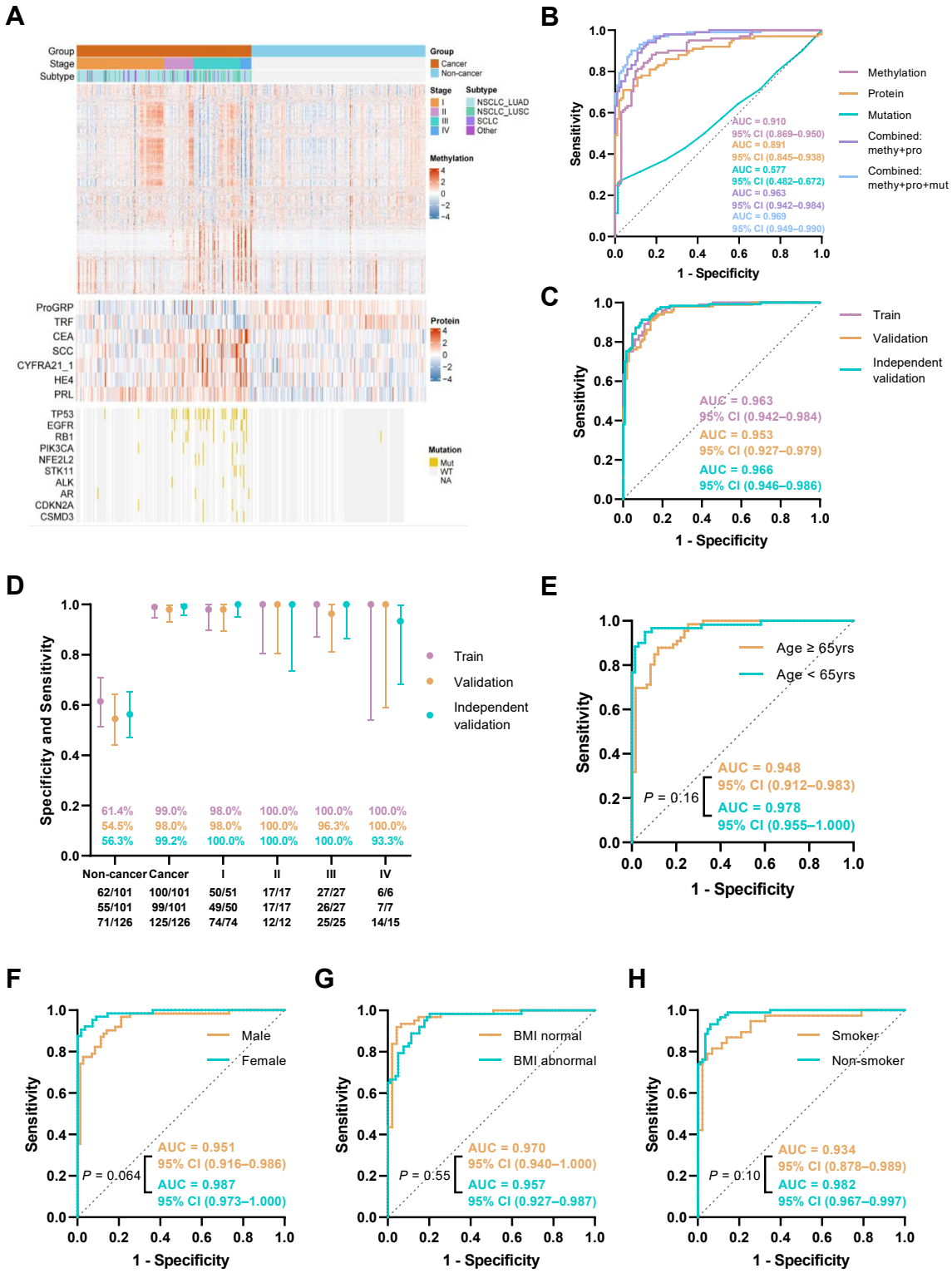

Fig. 3: **Performance of the lung cancer screening model.** **(A)** Heatmap of selected cfDNA methylation markers, mutations, protein features in cancer and non-cancer control blood samples of train (n = 202; cancer = 101; non-cancer control = 101) and validation (n = 202; cancer = 101; non-cancer control = 101) cohorts. **(B)** The receiver operating characteristic curves display the classification performance of single-omic models and multi-omics combined model in the train cohort (n = 202; cancer = 101; non-cancer control = 101). **(C)** The receiver operating characteristic curves

VA model (29.9% [95% CI, 22.1%–38.7%]), and three clinical experts' judgement (0.7%–10.4%). Furthermore, the AI-aided pulmonary nodules diagnostic model showed a lower fraction of benign diseases that would potentially receive invasive biopsy or surgery (24.0% [95% CI, 9.4%–45.1%]) compared to the Mayo model (28.0% [95% CI, 12.1%–49.4%]), the VA model (48.0% [95% CI, 27.8%–68.7%]), and three clinical experts' judgement (20.1%–36.1%). For user access, the diagnostic model will be made available online. A screenshot was provided in Supplementary Fig. S2. Doctors can estimate the risk level for pulmonary nodules by uploading CT and cfDNA methylation data. Pulmonary nodules with high-risk will be recommended for timely surgery or biopsy, while those with intermediate-risk or low-risk will be recommended for follow-up.

Exploratory association analysis of multi-omics in tissues

In the overall cancer patients with plasma ctDNA mutation data, ctDNA mutations were detected in 28.7% (54/188) patients (Supplementary Fig. S3A). The ctDNA mutation status were significantly associated with 1213 lung cancer specific DMRs as depicted in the heatmap (Supplementary Fig. S3B), exhibiting different methylation patterns between tumor-shed and tumor non-shed cancers. GO enrichment analysis showed hypermethylated (Supplementary Fig. S3C) and hypomethylated (Supplementary Fig. S3D) genes were enriched in different pathways. Moreover, out of the total cancer patients, 118 had tissue mutation data (Supplementary Fig. S3E), and among them, 92 also had paired plasma ctDNA mutation data. Notably, only 13 ctDNA mutations were detectable out of the 92 cancers with both paired tissue and plasma DNA sequencing data (Supplementary Fig. S3F), indicating that most of cancers were ctDNA mutation non-shedders.

In the analysis of mRNA sequencing data from 75 cancer tissue samples and 34 adjacent tissue samples (Supplementary Fig. S4A), it was observed that 1300 genes exhibited significant upregulation (Supplementary Fig. S4B) which were mainly enriched in organelle fission and nuclear division pathways (Supplementary Fig. S4C), while 697 genes displayed significant downregulation (Supplementary Fig. S4B) which were mainly enriched in ameboidal-type cell migration and regulation of vasculature development pathways (Supplementary Fig. S4D). The mRNA immune-cluster analysis revealed distinct immune subgroups as showed in Supplementary Fig. S4E.

Further analysis was conducted on the four DMRs commonly used in the lung cancer screening model and the AI-aided pulmonary nodules diagnostic model (Supplementary Table S5). The methylation level of the four DMRs between cancer and adjacent tissues was presented in Supplementary Fig. S5A, while mRNA expression of the four corresponding genes were showed in Supplementary Fig. S5B. In the association analysis of mRNA sequencing data and DNA methylation data from 75 cancer tissue samples and 34 adjacent tissue samples, it was discovered that the four DMRs showed a significantly negative association with the mRNA expression of the respective genes (Supplementary Fig. S5C). Meanwhile, the mRNA expression of four genes were primarily associated with the upregulation of notch signaling, hedgehog signaling, and wnt-beta-catenin signaling pathways, while the PI3K/AKT/mTOR signaling pathway was downregulated (Supplementary Fig. S5D). Moreover, notable correlations were observed between the mRNA expression of these four genes and immune cell enrichment, indicating an immune activation signature (Supplementary Fig. S5E).

Discussion

In this study, to address the issues of low compliance, high false-positive rates, and the potential radiation exposure associated with LDCT for lung cancer screening and post-screening pulmonary nodules management, we have developed a liquid biopsy-based comprehensive system called PKU-LCSMS. This system integrates two separate scenarios: a lung cancer screening model and an AI-aided pulmonary nodules diagnostic model, with blood cfDNA methylation as the central component. Utilizing the lung cancer screening

of the lung cancer screening model in the train (n = 202; cancer = 101; non-cancer control = 101), validation (n = 202; cancer = 101; non-cancer control = 101) and independent validation (n = 252; cancer = 126; non-cancer control = 126) cohorts, respectively. **(D)** Specificity and sensitivity with 95% confidence intervals of the lung cancer screening model in the train, validation and independent validation cohorts, respectively. The specificity was 61.4% (95% CI, 51.2%–70.9%), 54.5% (95% CI, 44.2%–64.4%), and 56.3% (95% CI, 47.2%–65.2%) in the train, validation, and independent validation cohorts, respectively. The sensitivity was 99.0% (95% CI, 94.6%–100%), 98.0% (95% CI, 93.0%–99.8%), and 99.2% (95% CI, 95.7%–100%) in the train, validation, and independent validation cohorts, respectively. The sensitivity was 98.0% (95% CI, 89.6%–100%) in stage I, 100% (95% CI, 80.5%–100%) in stage II, 100% (95% CI, 87.2%–100%) in stage III, and 100.0% (95% CI, 54.1%–100%) in stage IV in the train cohort. The sensitivity was 98.0% (95% CI, 89.4%–99.9%) in stage I, 100% (95% CI, 80.5%–100%) in stage II, 96.3% (95% CI, 81.0%–99.9%) in stage III, and 100.0% (95% CI, 59.0%–100%) in stage IV in the validation cohort. The sensitivity was 100.0% (95% CI, 95.1%–100%) in stage I, 100% (95% CI, 73.5%–100%) in stage II, 100% (95% CI, 86.3%–100%) in stage III, and 93.3% (95% CI, 68.1%–100%) in stage IV in the independent validation cohort. The bars **(E–H)** ROC curve of the age subgroup **(E)**, sex subgroup **(F)**, BMI subgroup **(G)**, and smoking status subgroup **(H)**. AUC, area under the curve. The *P* values for the statistical comparison of AUCs were obtained using the DeLong's test.

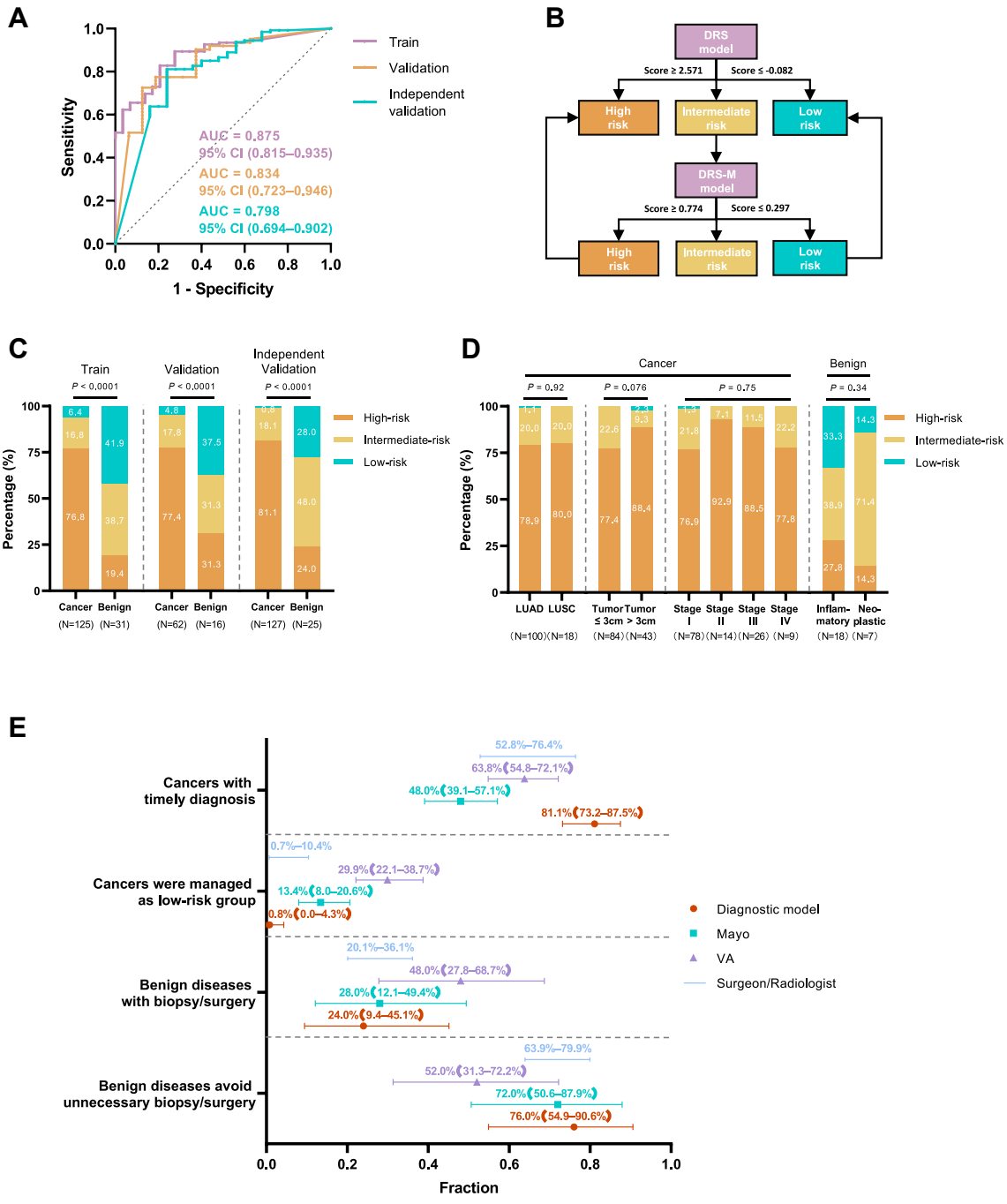

Fig. 4: **Performance of the AI-aided pulmonary nodules diagnostic model**. **(A)** The receiver operating characteristic curves display the classification performance of the AI-aided pulmonary nodules diagnostic model in the train, validation, and independent validation cohorts, respectively. **(B)** The workflow diagram of the AI-aided pulmonary nodules diagnostic model using the hierarchical fusion method. **(C)** Three category classifications of the AI-aided pulmonary nodules diagnostic model in the train (n = 156; cancer = 125, benign = 31), validation (n = 78; cancer = 62, benign = 16) and independent validation (n = 152; cancer = 127, benign = 25) cohorts. **(D)** Three category classifications of the AI-aided pulmonary nodules diagnostic model according to histology subtypes, tumor size, cancer stages, and subtypes of benign diseases in the independent validation cohort (n = 152; cancer = 127, benign = 25). **(E)** The potential clinical effect of three category classifications by the AI-aided pulmonary nodules diagnostic model, compared with Mayo model, VA model, and experts' judgement (two surgeons and one radiologist) in the independent validation cohort (n = 152; cancer = 127, benign = 25). The 95% confidence intervals were provided for the AI-aided pulmonary nodules diagnostic model, Mayo model, and VA model. The ranges were showed based on experts' judgement. All *P* values were obtained using the Fisher's exact test. AI, artificial intelligence; LUAD, lung adenocarcinoma; LUSC, lung squamous cell carcinoma; VA, Veterans Affairs.

model as a pre-screening step before LDCT, 56.3% of individuals may potentially avoid LDCT examination, with only a 0.8% chance of missing cancer who would receive a blood test next year for potential identification. Additionally, utilizing the AI-aided pulmonary nodules diagnostic model during the post-screening pulmonary nodules management phase, 81.1% of cancer patients would receive timely diagnoses and treatment. Only 0.8% of cancer patients would be classified as low-risk who would receive annual follow-up, while 76.0% of individuals with benign diseases could avoid invasive interventions. Specifically, the baseline blood test used for screening can also serve for subsequent post-screening management of pulmonary nodules, ensuring a convenient and efficient process throughout.

Following the National Comprehensive Cancer Network (NCCN) guidelines, individuals aged over 55 years old with a history of smoking exceeding 20 pack-years are classified as high risk population. They are strongly recommended to undergo annual LDCT screening for lung cancer and if suspicious lesions are detected, a professional medical evaluation is necessary to determine further diagnosis and treatment. This process comprises two essential parts: lung cancer screening and post-screening diagnostic assessment for pulmonary nodules. However, previous studies only targeted specific populations in one specific scenarios,[8,9,21,34] making it challenging to ascertain the universal applicability of their methods across these two distinct phases. This study represents a pioneering effort in the application of liquid biopsy to the existed two essential phases, which is primarily based on LDCT. We proposed the comprehensive lung cancer screening system called PKU-LCSMS, which integrated a multi-omics model based on cfDNA methylation and protein features for lung cancer screening, and an AI-aided diagnostic model based on radiomics and cfDNA methylation features for the discrimination between benign and malignant nodules. Four shared blood cfDNA methylation markers between screening and diagnosis were verified in tumor tissue, which are associated with an immune activation signature and the upregulation of the notch signaling pathway. In the independent validation cohort, both the multi-omics screening model and the AI-aided diagnostic model demonstrated a promising performance. These findings suggest that the potential benefits of implementing the PKU-LCSMS in high-risk populations, as it can precisely identify specific populations requiring clinical intervention and greatly enhance the identification, diagnosis, and management of lung cancer in these individuals.

Regarding the drawbacks of LDCT screening, such as high false-positive rates, limited imaging facilities, and low compliance rates, our noninvasive plasma method shows high sensitivity, especially in early-stage lung cancer, which can be complement to LDCT. Blood collection can be conveniently done locally at a clinic or through a home visit. Moreover, only individuals identified as high-risk based on the blood test are recommended to undergo LDCT. The multi-omics lung cancer screening model has undergone rigorous marker selection based on tissue samples, model development, and validation to ensure the robustness, distinguishing it from previous cfDNA methylation studies in lung cancer. Notably, across our three cohort, 68.0% of the participants diagnosed with early-stage lung cancer (stage I or II), which are amenable to curative surgical resection. A previously published plasma cfDNA-fragment-detection model called DELFI score, which was used before LDCT screening, achieved a sensitivity of 50–60% in stage I at a specificity of 80%.[9] Another ctDNA-based lung cancer detection model known as Lung-CLiP employing CAPP-Seq, achieved a sensitivity of 42% for stage I and 67% for stage II, with a notably high specificity of 98%.[8] While our priority in developing the screening model was to ensure high sensitivity to enrich the high-risk population for LDCT, thus minimizing the risk of missing lung cancer patients and avoiding the number of unnecessary LDCT, a certain degree of specificity was sacrificed. The screening model demonstrated excellent performance in detecting early-stage lung cancer (sensitivity: stage I, 100%; stage II, 100%) at the specificity of 56.3% in the independent validation cohort. In this study, the multi-omics screening model would be more generalizable and applicable in clinical practice, especially with its high sensitivity when used prior to LDCT. This is particularly crucial in reducing missed diagnoses and achieving favorable outcomes, especially in early-stage lung cancers.

Various technologies and entities of liquid biopsy demonstrate distinct strengths and weaknesses. For the lung cancer screening model in this study, the top classifiers by AUC were cfDNA methylation (0.910), serum protein (0.891), and ctDNA mutation (0.577). Furthermore, the performance was significantly improved when cfDNA methylation was combined with protein, resulting in an enhanced AUC of 0.963. However, the further enhancement is limited when all three-omics were combined (0.969). Although both cfDNA methylation and ctDNA mutation were features derived from cfDNA, cfDNA methylation demonstrated superior detection performance, consistent with comparison results reported in another study.[35] This can be attributed to the methylation's relatively abundant signals and lower limit of detection (LOD).[35] On the other hand, to rigorously eliminate the confounding factor of mutations related to clonal hematopoiesis, ctDNA mutations were sequenced using the UMI-tagged method at a depth of 35,000X, which was matched to the 10,000X depth sequencing with WBC in this study. However, in cancer cases where both tissue and plasma DNA mutation sequencing were conducted, only 14% (13 out of

92) showed detectable ctDNA. This indicates the constrained release of mutation signals into the bloodstream, potentially hindering its sensitivity. Consequently, the ctDNA mutation features were not included in the combination model. Intriguingly, with the added contribution of protein, it is reasonable to suggest that protein features originating from the serum level, could potentially complement DNA features for cancer detection. Nowadays, several lung cancer-specific protein panels have shown promise in the context of lung cancer screening.[14,15] It is also worth further investigating whether combining optimized protein panels with methylation markers can further enhance the overall performance.

In our study, the second primary aim was to effectively differentiate malignant pulmonary nodules from benign nodules, in order to minimize unnecessary invasive diagnostic biopsies or surgeries following lung cancer screening. To achieve this, we have developed an AI-aided pulmonary nodules diagnostic model using a sequential approach. This model combines radiomics and cfDNA methylations features that are generated during the initial screening phase, with no additional examination indeed. In clinical practice, the determination of tumor nature as benign or malignant is often reliant on the subjective judgment and experience of doctors, which can introduce variability and impact the accuracy of the results. Misdiagnosis leading to unnecessary surgical removal is a concern in clinical practice. The diagnostic model, which is not influenced by human factors in contrast to LDCT, demonstrates a sensitivity of 81.1% with a relatively high specificity (72.0%). In the lung screening phase, we tend to prioritize a strategy with higher sensitivity to minimize the possibility of cancer misdiagnosis when used before LDCT. However, in post-screening pulmonary nodules management phase, we aim for relatively higher balance of specificity and sensitivity to ensure accurate cancer detection while reducing unnecessary interventions for benign conditions. This differs from a previous study that used a specificity of only 50%.[34] The diagnostic model can help facilitate definitive diagnosis based on LDCT, minimizing the risk of unnecessary surgeries while ensuring accurate identification of malignant nodules. By reducing false positives and improving specificity, the diagnostic model offers potential benefits in optimizing patient management and decision-making in cases of suspected lung cancer. The result of diagnostic model have manifested more accurate decision-making for individuals in our cohort compared to traditional pulmonary nodule models, including Mayo model and VA model, as well as judgement by experienced doctors.

Overfitting is a common issue when utilizing machine learning methods for model construction in case–control studies. Given the large number of features used for model construction in this study, the current sample size falls significantly below the traditional requirements.[36] To mitigate overfitting, we employed the following methods: i) we first conducted feature selection based on tissue sequencing data; ii) we chose the linear kernel function when modeling with SVM to reduce model complexity; iii) we employed cross-validation to optimize model performance; iv) we introduced an independent validation cohort to evaluate the model's performance stability. The results indicated a marginal improvement in the lung cancer screening model's performance within the independent validation cohort, potentially influenced by a higher percentage of stage IV cancer cases (12%) compared to the train (6%) and validation (7%) cohorts. However, the performance of the AI-aided pulmonary nodules diagnostic model exhibited a slight decrease, possibly attributed to the limited sample size of benign cases, which could have led to potential overfitting. Further validation and follow-up studies with larger sample sizes will be imperative.

Several limitations should be acknowledged in this study. Firstly, the sample size may be insufficient, particularly when employing a multitude of features in machine learning, especially for benign cases. Despite relatively consistent performances being demonstrated in the independent validation cohort, the 95% CIs for sensitivity and specificity were wide, suggesting uncertainty of the findings. Further validation with larger sample sizes will be imperative. Secondly, smoking status were not taken into account during the stratification of the cancer and non-cancer control groups. Nevertheless, the smoking rates were comparable across the subgroups. Thirdly, the non-cancer controls were sourced from a separate study, which renders the independent validation cohort not entirely rigorously independent. Moreover, these non-cancer controls were not predominantly high-risk individuals for lung cancer screening. Fourthly, the methylation data of these overlapping cancer cases were used for the lung cancer screening model, while both methylation and radiomics data were used for the AI-aided pulmonary nodules diagnostic model. This overlap may potentially pose risks on affecting the reliability, generalizability, and stability of the PKU-LCSMS since if there are potential bias of these cancer cases, both models would be affected. However, these overlapping cancer cases also mimic the future clinical application scenario where the same cancer patients would first be identified by the lung cancer screening model and then be differentiated from benign nodules by the AI-aided pulmonary nodules diagnostic model. Finally, although we incorporated an independent validation cohort to assess the robustness of our findings, further validation and real-world implementation of the PKU-LCSMS remain essential to comprehensively assess its performance and influence on patient outcomes. While the baseline blood test can be utilized for both the screening and

subsequent post-screening management of pulmonary nodules, the presence of this integrated system with two models may increase the complexity of clinical translation. Specifically, the comparison of the model's performance against existing classical models should also be cautiously evaluated. The optimal follow-up interval for patients classified as low-risk or intermediate-risk has yet to be determined. A long-term follow-up study is also needed to refine the recommendations for clinical use of the PKU-LCSMS system in the screening and diagnostic scenarios.

Collectively, we have developed a comprehensive lung cancer screening and post-screening pulmonary nodules management system called PKU-LCSMS. This innovative system achieves a thorough evaluation of the entire process by integrating a multi-omics liquid biopsy model for pre-LDCT screening with high sensitivity and a diagnostic model based on chest CT images and cfDNA methylation for classification of pulmonary nodules after screening. With baseline blood sample as a core component, the integration of the screening phase and the post-screening management phase in the PKU-LCSMS offers a promising solution for lung cancer screening and post-screening management in the future.

Contributors

Yichen Jin, Wei Mu, and Yezhen Shi accessed and verified the data. Yichen Jin, Qingyi Qi, Wenxiang Wang, Yue He, and Yuxia Liu performed the experiments. Yezhen Shi and Bo Yang performed the data analyses and played a crucial role in the lung cancer screening model's development and validation. Wei Mu, Shuaitong Zhang, and Caifang Cao performed the data analyses and played a crucial role in the AI-aided pulmonary nodule diagnostic model's development and validation. Peng Cui analyzed the tissue sequencing data. Xiaoran Sun and Peng Cui generated informative visualizations and prepared the figures. Yuzi Zhang, Peng Cui, Chengcheng Li, Yezhen Shi, and Fang Liu wrote the manuscript text. Guoqiang Wang, Jing Zhao, and Yuzi Zhang helped performed the analysis with constructive discussions and edited the manuscript. Kezhong Chen, Fan Yang, Shangli Cai, and Jie Tian contributed to the conception of the study. All authors reviewed the manuscript.

Data sharing statement

The data that support the findings of this study are available on reasonable request from the corresponding authors.

Declaration of interests

Yezhen Shi, Xiaoran Sun, Bo Yang, Peng Cui, Chengcheng Li, Fang Liu, Yuxia Liu, Guoqiang Wang, Jing Zhao, Yuzi Zhang, and Shangli Cai are employees of Burning Rock Biotech.

Acknowledgements

This work was supported by Science, Technology & Innovation Project of Xiongan New Area (2023XAGG0071), Beijing Natural Science Foundation (L222021), CAMS Innovation Fund for Medical Sciences (CIFMS) 2022-I2M-C&T-B-120, Clinical Medicine Plus X-Young Scholars Project of Peking University, the Fundamental Research Funds for the Central Universities (PKU2023LCXQ008), Research Unit of Intelligence Diagnosis and Treatment in Early Non-small Cell Lung Cancer, Chinese Academy of Medical Sciences (2021RU002), National Natural Science Foundation of China (No.92059203, No.82388102, No.92259303, No.62176013), Peking University People's Hospital Research and Development Funds (RZ2022-03), National Key Research and Development Program of China (2022YFC2505105, 2022YFC2505106), and the Fundamental Research Funds for the Central Universities (No.YWF-20-BJ-J-1048).

Appendix A. Supplementary data

Supplementary data related to this article can be found at https://doi.org/10.1016/j.eclinm.2024.102769.

References

1 de Koning HJ, van der Aalst CM, de Jong PA, et al. Reduced lung-cancer mortality with volume CT screening in a randomized trial. *N Engl J Med*. 2020;382(6):503–513.
2 National Lung Screening Trial Research T, Aberle DR, Adams AM, et al. Reduced lung-cancer mortality with low-dose computed tomographic screening. *N Engl J Med*. 2011;365(5):395–409.
3 Wender RC, Brawley OW, Fedewa SA, Gansler T, Smith RA. A blueprint for cancer screening and early detection: advancing screening's contribution to cancer control. *CA Cancer J Clin*. 2019;69(1):50–79.
4 Gao Q, Zeng Q, Wang Z, et al. Circulating cell-free DNA for cancer early detection. *Innovation*. 2022;3(4):100259.
5 Heitzer E, Haque IS, Roberts CES, Speicher MR. Current and future perspectives of liquid biopsies in genomics-driven oncology. *Nat Rev Genet*. 2019;20(2):71–88.
6 Ignatiadis M, Sledge GW, Jeffrey SS. Liquid biopsy enters the clinic - implementation issues and future challenges. *Nat Rev Clin Oncol*. 2021;18(5):297–312.
7 Lone SN, Nisar S, Masoodi T, et al. Liquid biopsy: a step closer to transform diagnosis, prognosis and future of cancer treatments. *Mol Cancer*. 2022;21(1):79.
8 Chabon JJ, Hamilton EG, Kurtz DM, et al. Integrating genomic features for non-invasive early lung cancer detection. *Nature*. 2020;580(7802):245–251.
9 Cristiano S, Leal A, Phallen J, et al. Genome-wide cell-free DNA fragmentation in patients with cancer. *Nature*. 2019;570(7761):385–389.
10 Tao R, Cao W, Zhu F, et al. Liquid biopsies to distinguish malignant from benign pulmonary nodules. *Thorac Cancer*. 2021;12(11):1647–1655.
11 Haque IS. Enhanced DNA libraries for methylation analysis. *Nat Biomed Eng*. 2021;5(6):490–492.
12 Abbosh C, Birkbak NJ, Wilson GA, et al. Phylogenetic ctDNA analysis depicts early-stage lung cancer evolution. *Nature*. 2017;545(7655):446–451.
13 Nakamura H, Nishimura T. History, molecular features, and clinical importance of conventional serum biomarkers in lung cancer. *Surg Today*. 2017;47(9):1037–1059.
14 Davies MPA, Sato T, Ashoor H, et al. Plasma protein biomarkers for early prediction of lung cancer. *eBioMedicine*. 2023;93:104686.
15 Jett JR, Peek LJ, Fredericks L, Jewell W, Pingleton WW, Robertson JF. Audit of the autoantibody test, EarlyCDT(R)-lung, in 1600 patients: an evaluation of its performance in routine clinical practice. *Lung Cancer*. 2014;83(1):51–55.
16 Fehlmann T, Kahraman M, Ludwig N, et al. Evaluating the use of circulating MicroRNA profiles for lung cancer detection in symptomatic patients. *JAMA Oncol*. 2020;6(5):714–723.
17 Sikosek T, Horos R, Trudzinski F, et al. Early detection of lung cancer using small RNAs. *J Thorac Oncol*. 2023;18(11):1504–1523.
18 Kim DH, Park H, Choi YJ, et al. Identification of exosomal microRNA panel as diagnostic and prognostic biomarker for small cell lung cancer. *Biomark Res*. 2023;11(1):80.
19 Yang W, Qian F, Teng J, et al. Community-based lung cancer screening with low-dose CT in China: results of the baseline screening. *Lung Cancer*. 2018;117:20–26.
20 Gillies RJ, Kinahan PE, Hricak H. Radiomics: images are more than pictures, they are data. *Radiology*. 2016;278(2):563–577.
21 Mikhael PG, Wohlwend J, Yala A, et al. Sybil: a validated deep learning model to predict future lung cancer risk from a single low-dose chest computed tomography. *J Clin Oncol*. 2023;41(12):2191–2200.
22 Maldonado F, Varghese C, Rajagopalan S, et al. Validation of the BRODERS classifier (Benign versus aggRessive nODule Evaluation using Radiomic Stratification), a novel HRCT-based radiomic

classifier for indeterminate pulmonary nodules. *Eur Respir J*. 2021;57(4).
23 Beig N, Khorrami M, Alilou M, et al. Perinodular and intranodular radiomic features on lung CT images distinguish adenocarcinomas from granulomas. *Radiology*. 2019;290(3):783–792.
24 Hunter B, Chen M, Ratnakumar P, et al. A radiomics-based decision support tool improves lung cancer diagnosis in combination with the Herder score in large lung nodules. *eBioMedicine*. 2022;86:104344.
25 Kammer MN, Lakhani DA, Balar AB, et al. Integrated biomarkers for the management of indeterminate pulmonary nodules. *Am J Respir Crit Care Med*. 2021;204(11):1306–1316.
26 Michalak EM, Burr ML, Bannister AJ, Dawson MA. The roles of DNA, RNA and histone methylation in ageing and cancer. *Nat Rev Mol Cell Biol*. 2019;20(10):573–589.
27 Szymański P, Kajdanowicz T. In: Paula Branco Luís T, Nuno M, eds. *Proceedings of the first international workshop on learning with imbalanced domains: theory and applications. Proceedings of machine learning research*. PMLR; 2017:22–35.
28 Liang N, Li B, Jia Z, et al. Ultrasensitive detection of circulating tumour DNA via deep methylation sequencing aided by machine learning. *Nat Biomed Eng*. 2021;5(6):586–599.
29 Wang Z, Cheng Y, An T, et al. Detection of EGFR mutations in plasma circulating tumour DNA as a selection criterion for first-line gefitinib treatment in patients with advanced lung adenocarcinoma (BENEFIT): a phase 2, single-arm, multicentre clinical trial. *Lancet Respir Med*. 2018;6(9):681–690.
30 Newman AM, Lovejoy AF, Klass DM, et al. Integrated digital error suppression for improved detection of circulating tumor DNA. *Nat Biotechnol*. 2016;34(5):547–555.
31 Xie Y, Xia Y, Zhang J, et al. Knowledge-based collaborative deep learning for benign-malignant lung nodule classification on chest CT. *IEEE Trans Med Imaging*. 2019;38(4):991–1004.
32 Swensen SJ, Silverstein MD, Ilstrup DM, Schleck CD, Edell ES. The probability of malignancy in solitary pulmonary nodules. Application to small radiologically indeterminate nodules. *Arch Intern Med*. 1997;157(8):849–855.
33 Gould MK, Ananth L, Barnett PG, Veterans Affairs SCSG. A clinical model to estimate the pretest probability of lung cancer in patients with solitary pulmonary nodules. *Chest*. 2007;131(2):383–388.
34 He J, Wang B, Tao J, et al. Accurate classification of pulmonary nodules by a combined model of clinical, imaging, and cell-free DNA methylation biomarkers: a model development and external validation study. *Lancet Digit Health*. 2023;5(10):e647–e656.
35 Jamshidi A, Liu MC, Klein EA, et al. Evaluation of cell-free DNA approaches for multi-cancer early detection. *Cancer Cell*. 2022;40(12):1537–1549.e12.
36 Riley RD, Ensor J, Snell KIE, et al. Calculating the sample size required for developing a clinical prediction model. *BMJ*. 2020;368:m441.